ISSN 1070-3284, Russian Journal of Coordination Chemistry, 2016, Vol. 42, No. 6, pp. 410–417. © Pleiades Publishing, Ltd., 2016.

Syntheses, Crystal Structures, and Properties of Two Supramolecules Based on Methoxyphenyl Imidazole Dicarboxylates[1]

Y. L. Sang[a], *, J. F. Xin[a], and R. M. Gao[b]

[a] *College of Chemistry and Chemical Engineering, Chifeng University, Chifeng, 024000, Neimenggu, P.R. China*
[b] *College of Chemistry and Molecular Engineering, Zhengzhou University, Zhengzhou, 450001, Henan, P.R. China*
**e-mail: sangyali0814@126.com*

Received July 16, 2015

Abstract—Two cobalt(II) and cadmium(II) complexes, $[Co(H_2DMOPhIDC)_2(H_2O)_2] \cdot 2H_2O$ (H_3D-MOPhIDC = 2-(3,4-dimethoxyphenyl)-1*H*-imidazole-4,5-dicarboxylic acid) (**I**), $[Cd(H_2MOPhIDC)_2$-$(Phen)] \cdot C_2H_5OH$ ($H_3MOPhIDC$ = 2-(3-dimethoxyphenyl)-1*H*-imidazole-4,5-dicarboxylic acid, Phen = 1,10-phenanthroline) (**II**), have been hydro(solvo)thermally synthesized by employing two kinds of organic ligands, $H_3DMOPhIDC$ or $H_3MOPhIDC$, respectively. The molecular structures of **I** and **II** have been characterized by IR spectra, elemental analyses and single-crystal X-ray diffraction (CIF files CCDC nos. 935845 (**I**), 935846 (**II**)). Both complexes show three-dimensional supramolecular structures supported by intermolecular H-bonds. Furthermore, the thermogravimetric and photoluminescent properties of two complexes have been investigated as well.

DOI: 10.1134/S1070328416050079

INTRODUCTION

Recently, supramolecular complexes based on carboxylate-base compounds have attracted much attention due to their novel architectures and potential applications in functional material field [1–10]. In this context, imidazole-4,5-dicayboxylic acid (H_3IDC) is a good construction block for supramolecules due to its promising coordination ability and coordination modes.

To have a deep understanding of the coordination features of H_3IDC and its derivatives, a series of imidazole dicarboxylate ligands bearing 2-position aromatic groups have been synthesized and investigated [11–18]. For example, people have adopted methoxyl group to modify the phenyl unit at the 3-position or 3,4-positions, achieving two kinds of organic ligands: 2-(3-methoxyphenyl)-1*H*-imidazole-4,5-dicarboxylic acid (*m*-$H_3MOPhIDC$) and 2-(3,4-dimethoxyphenyl)-1*H*-imidazole-4,5-di-carboxylic acid (H_3D-MOPhIDC) [15]. The early studies showed that the ligands *m*-$H_3MOPhIDC$ and $H_3DMOPhIDC$ could be doubly deprotonated and coordinated to metal ions in various modes. Consequently, a series of intriguing MOFs, such as 3D $[Sr(m\text{-}H_2MOPhIDC)_2]_n$, 2D $[Cd_3(m\text{-}H_2MOPhIDC)_2(\mu_3\text{-}HMOPhIDC)_2(H_2O)_2]_n$ [14], 3D polymers $[Sr(3,4\text{-}H_2DMOPhIDC)_2]_n$ have been prepared [15]. Among these complexes, the two ligands have similar coordination modes: (1) acting as chelating ligand using one nitrogen atom and one carboxylate oxygen atom or using two carboxylate oxygen atoms; (2) acting as bridging ligand using two nitrogen atoms. Although some coordination polymers have been prepared, supramolecular complexes were rarely synthesized. We believe that the two organic ligands may supply intra- and intermolecular H-bonds, π–π stacking effects, and van der waals interactions, which play vital roles in the construction of supramolecular structures. The syntheses of complexes **I** and **II** are given below:

---

[1] The article is published in the original.

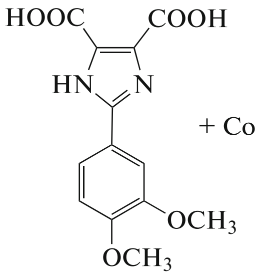

$$+ Co(NO_3)_2 \cdot 6H_2O \xrightarrow[150°C\ 96\ h]{H_2O} [Co(H_2DMOPhIDC)_2(H_2O)_2] \cdot 2H_2O \qquad \textbf{(I)}$$

$H_3DMOPhIDC$

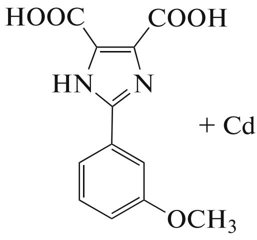

$$+ Cd(NO_3)_2 \cdot 4H_2O + Phen \xrightarrow[160°C\ 24\ h]{C_2H_5OH/H_2O} [Cd(H_2MOPhIDC)_2(Phen)_2] \cdot C_2H_5OH. \qquad \textbf{(II)}$$

$H_3MOPhIDC$

Considering above mentions, in this paper, two supramolecular complexes, namely $[Co(H_2DMOPhIDC)_2(H_2O)_2] \cdot H_2O$ (**I**), $[Cd(H_2MOPhIDC)_2(Phen)] \cdot CH_3CH_2OH$ (Phen = 1,10-phenanthroline) (**II**), have been hydro(solvo)thermally synthesized. Their thermal and fluorescence properties have been investigated as well.

EXPERIMENTAL

Materials and methods. All chemicals were of reagent grade quality obtained from commercial sources and used without further purification. The organic ligands H_3MOIDC and $H_3DMOPhIDC$ were prepared according to the literature method [19]. C, H, and N analyses were carried out on a FLASH EA 1112 analyzer (USA). IR data were recorded on a BRUKER TENSOR 27 spectrophotometer as KBr pellets in the 400–4000 cm^{-1} region (Germany). TG measurements were performed by heating the sample from 20 to 750°C at a rate of 10°C min^{-1} in air on a Netzsch STA 409PC differential thermal analyzer (Germany). Fluorescence spectra were characterized at room temperature by a F-4500 fluorescence spectrophotometer (Japan).

Synthesis of I. A mixture of $H_3DMOPhIDC$ (26.2 mg, 0.09 mmol), $Co(NO_3)_2 \cdot 6H_2O$ (29.1 mg, 0.1 mmol), Et_3N (0.028 mL, 0.2 mmol) and deionized water (7 mL) was sealed in a 25 mL Teflon-lined bomb and heated at 150°C for 4 days. The reaction mixture was then allowed to cool to room temperature. Reddish brown crystals of **I** were collected, washed with distilled water, and dried in air. The yield was 78%.

IR (KBr; ν, cm^{-1}): 3490 w, 2846 w, 2360 w, 1581 s, 1398 s, 1263 s, 1019 m, 865 w, 770 m, 723 m, 546 m.

For $C_{26}H_{30}N_4O_{16}Co$			
anal. calcd., %:	C, 43.73;	H, 4.2;	N, 7.85.
Found, %:	C, 43.88;	H, 3.87;	N, 7.76.

Synthesis of II. A mixture of $H_3MOPhIDC$ (52.4 mg, 0.2 mmol), $Cd(NO_3)_2 \cdot 4H_2O$ (61.6 mg, 0.2 mmol), Phen (39.6 mg, 0.2 mmol), Pyridine (0.224 mL, 1.6 mmol) and C_2H_5OH–H_2O (3 : 4, 7 mL) was sealed in a 25 mL Teflon-lined bomb, which was heated to 160°C for 1 day, and then cooled to room temperature. White crystals of **II** were obtained and dried in air. The yield was 70%.

IR (KBr; ν, cm–1): 3453 m, 3061 m, 1944 w, 1576 s, 1537 m, 1471 s, 1386 m, 1234 s, 1047 s, 846 s, 747 s, 728 s, 638 m.

For C38H32N6O11Cd			
anal. calcd., %:	C, 52.96;	H, 3.72;	N, 9.75.
Found, %:	C, 52.77;	H, 3.64;	N, 9.85.

X-ray crystallography. All measurements were made on a Bruker smart APEXII CCD diffractometer with a graphite-monochromated MoK_α radiation (λ = 0.71073 Å). Single crystals of **I** and **II** were selected and mounted on a glass fiber. All data were collected at a temperature of 291(2) K using the ω–2θ scan technique and corrected for Lorenz-polarization effects. Furthermore, a correction for secondary extinction was applied.

Table 1. Crystallographic data and structure refinement information for compounds **I** and **II**

Parameter	Value	
	I	**II**
Fw	713.47	861.10
Crystal system	Triclinic	Triclinic
Space group	$P\bar{1}$	$P\bar{1}$
Crystal size, mm	0.27 × 0.26 × 0.18	0.20 × 0.18 × 0.14
a, Å	9.033(3)	11.0034(4)
b, Å	10.621(4)	12.5774(4)
c, Å	15.615(5)	14.6687(5)
α, deg	95.951(5)	109.735(3)
β, deg	100.193(5)	105.922(3)
γ, deg	92.520(6)	93.063(3)
V, Å^3	1463.5(9)	1813.43(11)
Z	2	2
ρ_{calcd}, mg m^{-3}	1.619	1.577
F(000)	738	876
μ, mm^{-1}	0.673	5.439
Reflections mesured/unique	9765/6916	14293/6485
(R_{int})	(0.0226)	(0.0315)
Data/restraints/parameters	6916/470/436	6485/357/547
Goodness-of-fit on F^2	1.037	1.038
R, wR ($I > 2\sigma(I)$)	0.0612, 0.1607	0.0317, 0.0784
R, wR (all data)	0.0824, 0.1760	0.0374, 0.0820
$\Delta\rho_{max}/\Delta\rho_{min}$, e Å^{-3}	−1.442/1.130	−0.421/0.342

The two structures were solved by direct methods and expanded using the Fourier technique. The non-hydrogen atoms were refined with anisotropic thermal parameters. Hydrogen atoms were included but not refined. The final cycle of full-matrix least squares refinement was based on 6916 observed reflections and 436 variable parameters for **I**, and 6485 observed reflections and 547 variable parameters for **II**. All calculations were performed using the SHELX-97 crystallographic software package [20]. Crystal data and experimental details for compounds **I** and **II** are contained in Table 1. The selected bond lengths and angles and hydrogen bonding parameters are given in Tables 2 and 3, respectively.

Supplementary material for structures **I** and **II** has been deposited with the Cambridge Crystallographic Data Centre (nos. 935845 (**I**), 925846 (**II**); deposit@ccdc.cam.ac.uk or http://www.ccdc.cam.ac.uk).

RESULTS AND DISCUSSION

In general, under hydrothermal synthesis conditions the methoxyphenyl-substituted imidazole dicarboxylate ligand at 2-position usually shows various coordination modes and can reacts with metal ions to obtain relatively complicated coordination polymers or polynuclear complexes. However, in this article, two mononuclear complexes were obtained. For complex **I**, the results indicate that under the hydrothermal conditions, the factors controlling the reaction and supramolecular assembly are intricate, especially pH value. In the preparation of complex **I**, the crystal successfully grew from the solution of pH 5, while the higher pH value has failed to produce suitable crystal or has given products with low yields. In addition, the two mononuclear complexes are stable in air and insoluble in water and common organic solvents.

An ORTEP drawing of the molecular structure with atom labeling scheme is shown in Fig. 1. The geometry around the Co(II) center is best portrayed as a slightly distorted [CoO_4N_2] octahedral environment, which is defined by two nitrogen atom (N(1) and N(3)) and two carboxylate oxygen atoms (O(1) and O(10)) from two individual $H_2DMOPhIDC^-$ anions, and the remaining site is occupied by two oxygen atoms (O(13) and O(14)) from the two coordination water molecules (Fig. 1a). The O(10)CoO(13) and O(14)CoO(1) bond angles are 171.92(10)° and

Table 2. Selected bond distances (Å) and angles (deg) for complexes **I** and **II**

Bond	*d*, Å	Bond	*d*, Å	Bond	*d*, Å
		I			
Co(1)–O(14)	2.026(3)	Co(1)–O(13)	2.121(3)	Co(1)–O(1)	2.152(3)
Co(1)–O(10)	2.103(3)	Co(1)–N(1)	2.144(3)	Co(1)–N(3)	2.200(3)
		II			
Cd(1)–O(6)	2.269(2)	Cd(1)–N(6)	2.328(3)	Cd(1)–N(5)	2.377(2)
Cd(1)–O(1)	2.3137(19)	Cd(1)–N(1)	2.334(2)	Cd(1)–N(3)	2.381(2)
Angle	ω, deg	Angle	ω, deg	Angle	ω, deg
		I			
O(14)Co(1)O(10)	95.74(11)	O(13)Co(1)N(1)	86.26(10)	O(14)Co(1)N(3)	91.34(10)
O(14)Co(1)O(13)	92.22(11)	O(14)Co(1)O(1)	177.68(10)	O(10)Co(1)N(3)	78.81(10)
O(10)Co(1)O(13)	171.92(10)	O(10)Co(1)O(1)	85.77(10)	O(13)Co(1)N(3)	102.44(10)
O(14)Co(1)N(1)	102.76(11)	O(13)Co(1)O(1)	86.32(10)	N(1)Co(1)N(3)	163.22(11)
O(10)Co(1)N(1)	90.61(10)	N(1)Co(1)O(1)	78.96(10)	O(1)Co(1)N(3)	87.22(10)
		II			
O(6)Cd(1)O(1)	108.10(8)	N(6)Cd(1)N(1)	95.20(8)	O(6)Cd(1)N(3)	72.77(7)
O(6)Cd(1)N(6)	158.89(9)	O(6)Cd(1)N(5)	88.53(9)	O(1)Cd(1)N(3)	82.33(7)
O(1)Cd(1)N(6)	92.99(8)	O(1)Cd(1)N(5)	159.25(8)	N(6)Cd(1)N(3)	110.20(8)
O(6)Cd(1)N(1)	92.00(8)	N(6)Cd(1)N(5)	70.68(9)	N(1)Cd(1)N(3)	145.43(8)
O(1)Cd(1)N(1)	73.03(7)	N(1)Cd(1)N(5)	119.87(8)	N(5)Cd(1)N(3)	91.23(8)

Table 3. Geometric parameters of hydrogen bonds for **I** and **II***

D–H···A	Distance, Å			Angle DHA, deg
	D–H	H···A	D···A	
		I		
N(4)–H(4)···O(1)$^{\#1}$	0.86	2.10	2.914(4)	158
N(2)–H(2)···O(2*w*)	0.86	1.93	2.781(4)	173
O(13)–H(13*D*)···O(4)$^{\#2}$	0.85	1.96	2.771(4)	160
O(13)–H(13*E*)···O(7)$^{\#1}$	0.85	1.87	2.724(4)	178
O(14)–H(14*A*)···O(1*w*)	0.85	1.87	2.647(4)	152
O(1*w*)–H(1*wA*)···O(8)$^{\#4}$	0.85	2.03	2.875(4)	172
O(14)–H(14*B*)···O(6)$^{\#3}$	0.85	2.09	2.868(4)	152
O(1*w*)–H(1*wB*)···O(12)$^{\#5}$	0.85	2.13	2.976(4)	172
O(1*w*)–H(1*wB*)···O(11)$^{\#5}$	0.85	2.46	2.979(4)	120
O(2*w*)–H(2*wA*)···O(7)$^{\#6}$	0.85	2.23	3.038(4)	159
O(2*w*)–H(2*wB*)···O(10)$^{\#7}$	0.85	2.03	2.839(4)	158
		II		
O(3)–H(3)···O(2)	0.82	1.68	2.499(3)	179
O(8)–H(8)···O(7)	0.82	1.68	2.500(4)	179
N(2)–H(2)···O(11)$^{\#1}$	0.836(18)	2.025(19)	2.856(4)	173(3)
N(4)–H(4)···O(1)$^{\#2}$	0.82(4)	2.06(4)	2.851(3)	162(3)
O(11)–H(11*A*)···O(7)$^{\#3}$	0.82	2.20	2.977(4)	159
O(11)–H(11*A*)···O(6)$^{\#3}$	0.82	2.50	3.174(4)	141

* Symmetry transformations used to generate equivalent atoms: $^{\#1}$ $-x + 1, -y, -z$; $^{\#2}$ $-x + 1, -y, -z + 1$; $^{\#3}$ $-x + 2, -y + 1, -z + 1$; $^{\#4}$ $-x + 2, -y, -z$; $^{\#5}$ $-x + 1, -y + 1, -z$; $^{\#6}$ $x, y, z + 1$; $^{\#7}$ $-x + 2, -y, -z + 1$ for **I**; $^{\#1}$ $-x + 2, -y + 1, -z + 1$; $^{\#2}$ $-x, -y, -z$; $^{\#3}$ $x + 1, y, z$ for **II**.

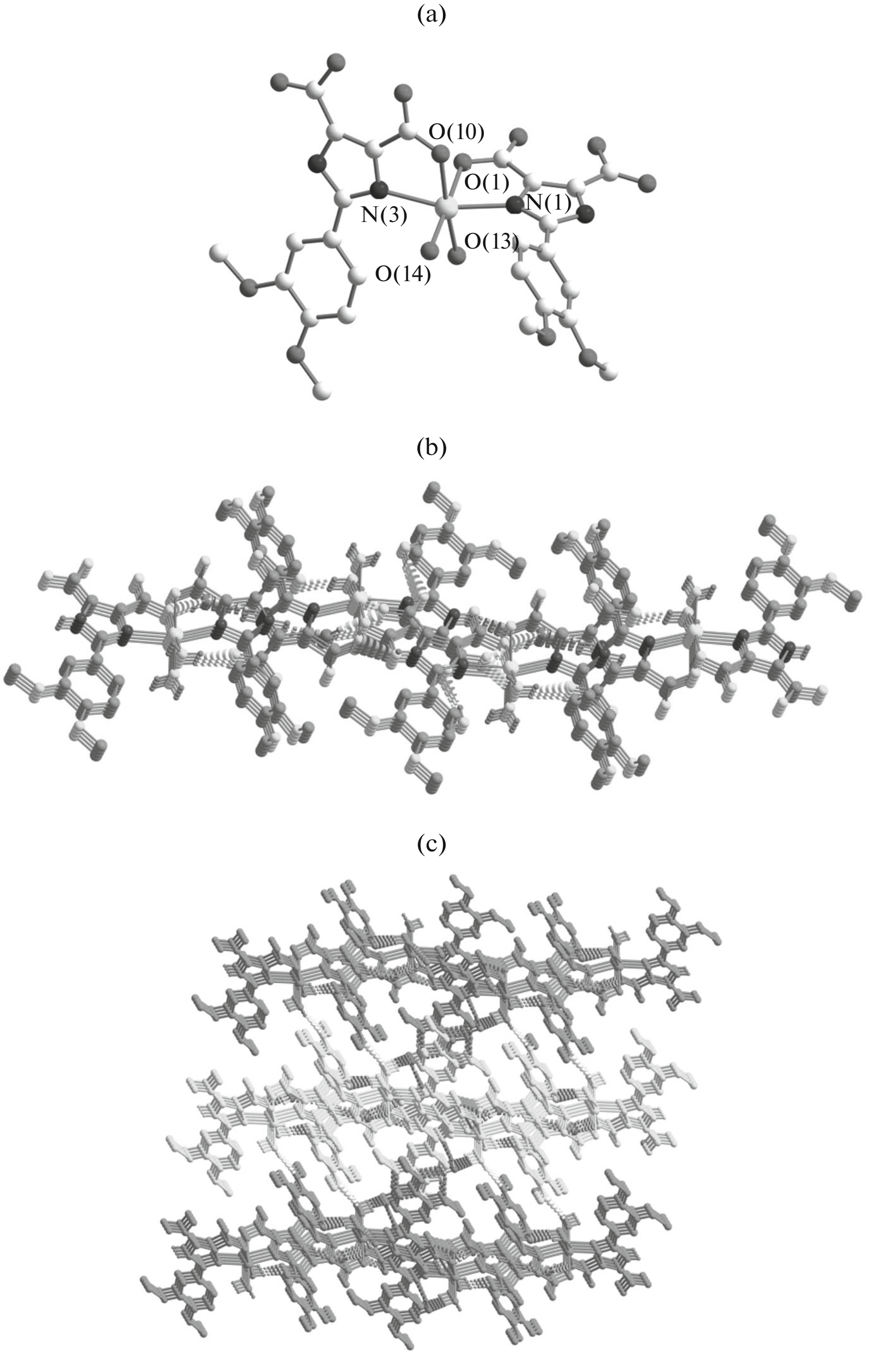

Fig. 1. Coordination arrangement of the Co atom of complex **I** (solvent removed) (a); the 2D layer composed via the intermolecular hydrogen bonds along the *x* axis of complex **I** (b); the solid-state crystal packing of complex **I** (c).

177.68(10)°, respectively. The O(1)CoO(13) and O(10)CoO(14) bond angles are 86.32(10)° and 95.74(11)°, respectively. Thus, the CoO_4 unit forms an ideal equatorial plane. Co–O(1) and Co–O(10) bond lengths (mean 2.127 Å) are longer than the Co–O(14) and Co–O(13) bond lengths (mean 2.074 Å). The Co–N bond lengths are 2.200(3) and 2.144(3) Å, respectively.

It should be pointed out that the H_3DMOPhIDC shows bidentate coordination mode. Within the organic ligand, the dihedral angle between the imidazole ring and the carboxylate plane is 11.147(175)° indicating the small twist. The dihedral angle between the two imidazole rings is 81.534°. The bond lengths and angles within the H_2DMOPhIDC$^-$ ligand are similar to these reported compounds [15].

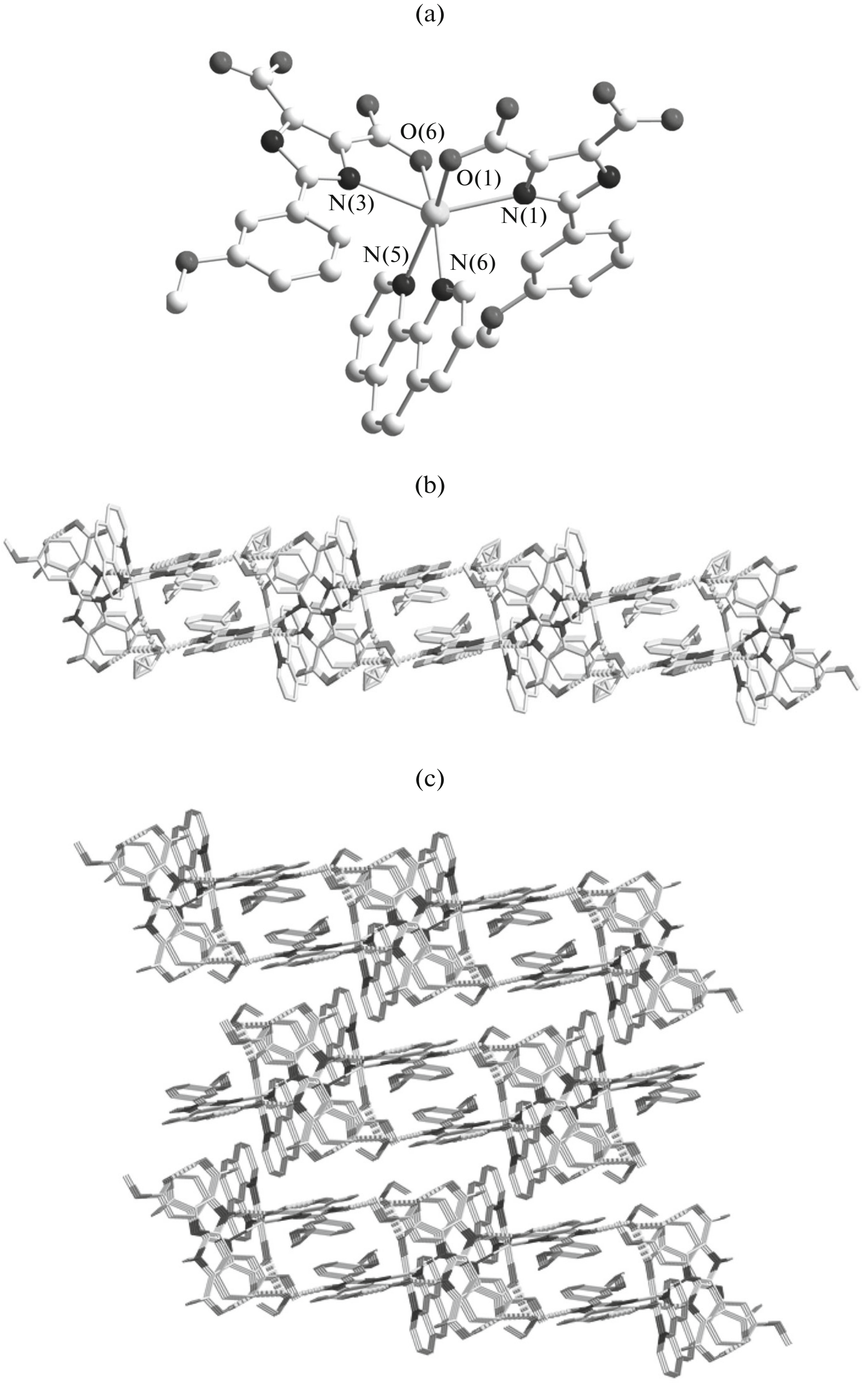

Fig. 2. Coordination arrangement of the Cd atom in complex **II** (solvent removed) (a); the zigzag chains of complex **II** (b); crystal packing diagram of complex **II** along the *y* axis showing the π–π stacking between the zigzag chains (c).

It should be point that both the $H_2DMOPhIDC^-$ units and water molecules participate in the formation of intermolecular hydrogen bonds O–H···O, N–H···O (Fig. 1b). H-bonds form 2D straight chains, and the intra-chain distance of adjacent Co^{2+} ions is 9.4354 and 10.0705 Å in turn. The 3D framework layer is constituted via the linkages of the hydrogen bonds between the adjacent chains. The structure indicated that one coordination water molecule connected adjacent $[Co(H_2DMOPhIDC)_2(H_2O)_2]$ units through two H-bonds like a bidentate ligand in the every 2D straight chain, while the other coordination water

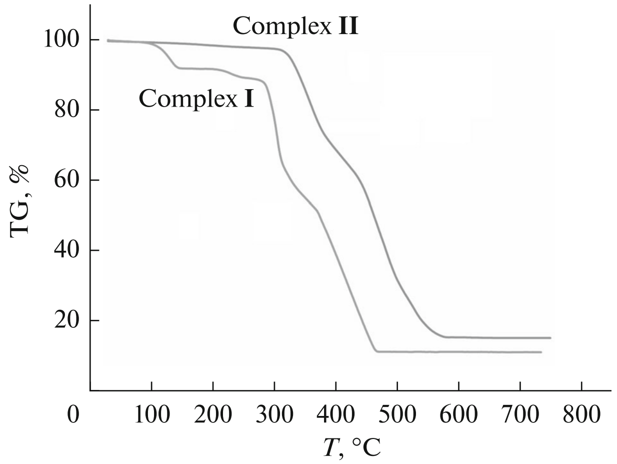

Fig. 3. TG curves of compounds **I** and **II**.

molecule acting as polydentate ligand joined the 2D straight chains through furcated H-bond. Furthermore, π···π stacking interactions of the phenyl rings also increased structural stability. To the best of our knowledge, the ligand $\mathrm{H_3DMOPhIDC}$ was first used to prepare Co complexes by us.

The Cd atoms of complex **II** is also six-coordinated like complex **I**. As is shown in Fig. 2, the $\mathrm{Cd^{2+}}$ ion is chelated by two $\mathrm{N_{phen}}$ donors (Cd–N(6) 2.328(3), Cd–N(5) 2.377(2) Å) and the $\mathrm{O^{-}_{H_2MOPhIDC}}$, $\mathrm{N^{-}_{H_2MOPhIDC}}$ chelating donors (the distances of Cd–O(1), Cd–N(1), Cd–O(6), and Cd–N(3) 2.3137(19), 2.334(2), 2.269(2), and 2.381(2) Å, respectively). Three stable five-membered rings were formed through Cd atoms and coordinated atoms. The coordination environment of $\mathrm{Cd^{2+}}$ ion is a seriously distorted octahedron. The Phen acts as a bidentate ligand to coordinate $\mathrm{Cd^{2+}}$ ion. The intramolecular hydrogen bonds O–H···O are formed by oxygen atoms of carboxyl (O(3), O(2)) and (O(8), O(7)) of the imidazole dicarboxylate units, respectively, and the intermolecular hydrogen bonds N–H···O, O–H···O connect cadmium atoms to form a zigzag chain. In addition to the H-bonds mentioned above, the adjacent parallel helices assemble a 3D structure through weak π–π stacking (the distance and dihedral between the two staggered phen rings is 4.8781 Å and 0°). Both of them supply the stability effect for the 3D solid-state structure of complex **II** [12].

As far as we konw, there are some imidazole–dicarboxylate-based Cd(II) coordination polymers in the literature, which are mainly built by $\mathrm{H_3IDC}$ or its 2-position substituted derivatives, respectively. There are only several examples of Cd(II) supramolecules, which are prepared from the methoxylphenyl substituted imidazole dicarboxylate ligands at 2-position.

The IR spectra of compounds **I** and **II** display characteristic absorption bands for water molecules, imidazole, carboxylate, and phenyl units. The strong and broad absorption bands in the range of 3400–3500 $\mathrm{cm^{-1}}$ should be ascribed to the stretching vibrations ν(N–H) and the ν(O–H), which indicate the presence of the imidazole ring and coordinated water molecules, respectively. The carboxylate units can be seen from the absorption bands in the frequency range 1234–1944 $\mathrm{cm^{-1}}$ in complexes owing to $\nu_{as}(\mathrm{COO^-})$ and $\nu_s(\mathrm{COO^-})$ vibrations respectively. The absorption in the range of 1000–1390 $\mathrm{cm^{-1}}$ are attributed to C=N and C=C vibrations. The characteristic IR band of the phenyl ring at 840–860 $\mathrm{cm^{-1}}$ due to δ(CH) vibrations can be found at 865 $\mathrm{cm^{-1}}$ for **I** and 846 $\mathrm{cm^{-1}}$ for **II**. In conclusion, the infrared spectral data (400–4000 $\mathrm{cm^{-1}}$) of two complexes are consistent with crystal structure analyses.

TG curve of complex **I** shows three-step weight loss process (Fig. 3). Complex **I** is stable until 99.3°C, then the first and the second lose weight from 99.3 to 281.1°C, the total weight loss of the both steps is 11.12% (calcd. 10.0%); they are corresponding to release of two crystallization water molecule and two coordination water molecules. The third weight loss step is from 281.1 to 465.4°C, the total weight loss of the both steps is 77.39% (calcd. 77.36%), which corresponds to the decomposition of the organic ligands. Finally, a plateau region is observed from 465.4 to 750°C. A nigger-brown amorphous residue is $\mathrm{0.5Co_2O_3}$ (obsd. 11.49%, calcd. 11.62%).

TG curve of complex **II** shows three-step weight loss process (Fig. 3). The complex is stable until 115.2°C, then the first step loses weight from 115.2 to 326.7°C (obsd. 3.04%, calcd. 5.3%) corresponding to losses of crystallization ethanol molecules. The second weight loss step is from 326.7 to 359.8°C which can attribute to the release of the COOH and $\mathrm{OCH_3}$ groups (obsd. 18.85%, calcd. 17.65%). On further heating, we observed the third a weight loss of 62.37% between 359.8 and 570.1°C (calcd. 63.94%), revealing the loss of the decomposition of Phen and the part $\mathrm{H_2MOPhIDC^-}$ ligands. The residue is stable up to about 570°C with the remaining weight of 15.73%, revealing the formation of CdO (calcd. 14.91%).

The fluorescence properties of complexes **I**, **II** and the corresponding ligand $\mathrm{H_3MOPhIDC}$ were examined in the solid state at room temperature (Fig. 4). Compound **I** shows luminescence with the emission maximum at 400 nm by selective excitation at 494 nm, which is attributed to the $\pi^* \rightarrow n$ transition. The emission can be assigned to the ligand-to-metal charge transfer (LMCT), rather than the $\pi^* \rightarrow n$ transition of the ligand [21]. In the case of compound **II,** the emission band with a maximum at 452 nm upon excitation at 347 nm was observed. The emission peaks of **II** are neither metal-to-ligand charge transfer (MLCT) nor

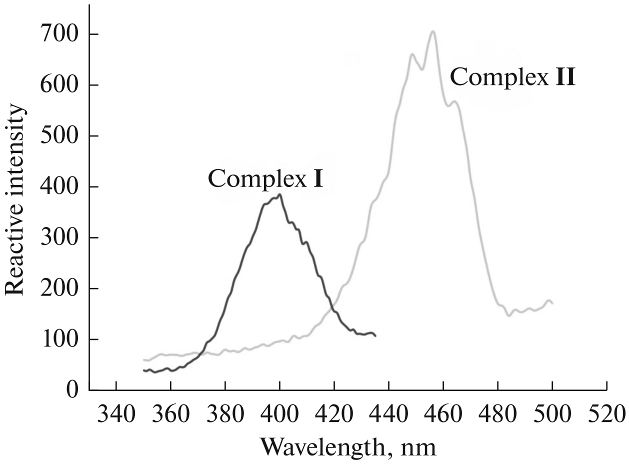

Fig. 4. The fluorescent spectra of complexes **I** and **II**.

ligand-to-metal charge transfer (LMCT) in nature. Because Cd^{2+} ions are difficult to reduce to their d^{10} configuration. This phenomenon can be tentatively assigned to intraligand transfer π^*–π transitions, namely, ligand-to-ligand charge transfer (LLCT), similar to the results reported on coordination polymers with an aromatic backbone.

ACKNOWLEDGMENTS

We gratefully acknowledge the financial support by the Research Program of Science and Technology at Universities of Inner Mongolia Autonomous Region (NJZY239) and Inner Mongolia Key Laboratory of Photoelectric Functional Materials.

REFERENCES

1. Guha, S., Drew, M.G.B., and Banerjee, A., *Cryst. Growth Des.*, 2010, vol. 10, p. 4716.
2. Chen, S.P., Hu, L., Hu, X.J., et al., *Cryst. Growth Des.*, 2009, vol. 9, p. 3835.
3. Lu, Z.L., Gamez, P., Mutikainen, I., et al., *Cryst. Growth Des.*, 2007, vol. 7, p. 1669.
4. Dong, S.Y., Zheng, B., Zhang, M.M., et al., *Macromolecules*, 2012, vol. 45, p. 9070.
5. Li, S.S., Yan, H.J., Wan, L.J., et al., *J. Am. Chem. Soc.*, 2007, vol. 129, p. 9268.
6. Ji, X.F., Yao, Y., Li, J.Y., et al., *J. Am. Chem. Soc.*, 2013, vol. 135, p. 74.
7. Ma, D., Tu, K., and Zhang, L.M., *Biomacromolecules*, 2010, vol. 11, p. 2204.
8. Moulton, B. and Zaworotko, M.J., *Chem. Rev.*, 2001, vol. 101, p. 1629.
9. Ferey, G., Mellot-Draznieks, C., Serre, C., et al., *Chem. Rev.*, 2005, vol. 105, p. 217.
10. Ockwig, N.W., Delgado-Friedrichs, O., O'Keeffe, M., et al., *Chem. Rev.*, 2005, vol. 105, p. 176.
11. Li, Z.F., Luo, X.B., Gao, Y.C., et al., *Inorg. Chim. Acta*, 2012, vol. 384, p. 352.
12. Zhang, Y., Luo, X.B., Yang, Z.L., et al., *CrystEngComm*, 2012, vol. 14, p. 7382.
13. Wang, C.J., Wang, T., Li, L., et al., *Dalton Trans.*, 2013, vol. 42, p. 1715.
14. Xiong, Z.F., Gao, R.M., Xie, Z.K., et al., *Dalton Trans.*, 2013, vol. 42, p. 4613.
15. Xiong, Z.F., Shi, B.B., Zhang, M.M., et al., *CrystEngComm*, 2013, vol. 15, p. 4885.
16. Zhang, Y., Guo, B.B., Li, L., et al., *Cryst. Growth Des.*, 2013, vol. 13, p. 367.
17. Guo, M.W., Chen, N., Yue, Z.F., et al., *CrystEngComm*, 2012, vol. 14, p. 4955.
18. Wang, W.Y., Yang, Z.L., Wang, C.J., et al., *CrystEngComm*, 2011, vol. 13, p. 4895.
19. Lebedev, A.V., Lebedeva, A.B., Sheludyakov, V.D., et al., *Russ. J. Gen. Chem.*, 2007, vol. 77, p. 855.
20. Sheldrick, G.M., *SHELX-97*, Göttingen: Univ. of Göttingen, 1997.
21. Yue, S.T., Wei, Z.Q., Liu, W.N., et al., *Inorg. Chem. Commun.*, 2012, vol. 14, p. 1396.